APPLICATION OF STATE TRANSITION MATRIX TO PARTICLE FLOW CT IMAGES

Masahiro TAKEI*, Mitsuaki OCHI*2, Yoshifuru SAITO*3 and Kiyoshi HORII*4
* Nihon University, Tokyo, Japan, takei@mech.cst.nihon-u.ac.jp,
*2 Hosei University, Tokyo Japan
*3 Shirayuri College, Tokyo Japan

Keywords: *Transition matrix, Capacitance CT, Free fall particles, Image processing*

ABSTRACT

Spatial particle density distribution images in a pipe cross-section have been evaluated by means of state transition matrix, which is a parameter indicating the dominant particle density transition patterns among time series images consisting of CT 2D-space and 1D-time. State transition characterizes the transition patterns for positions in a cross-section as monotonous transitions, sudden transitions, and extreme value transitions. In coarse and fine free-fall particles in a vertical pipe, A high, sudden and extreme value transitions occur near the pipe center when the particle flow rate is high, because the probability of collision among particles is high. Moreover, sudden and extreme value transitions in the case of fine particles is more diffused on a cross section than those in the case of coarse particles.

1 INTRODUCTION

Movements of particles, powders, and granules have been scrutinized in an effort to attain high performance operation in chemical engineering facilities such as air transportation equipment and circulating fluidized beds. For example, particle density distribution in particle-laden turbulent channel flow was measured by the Laser sheet method [1], and the distribution in channel flow was calculated by Large eddy simulation [2]. Moreover, total particle density at a pipe center line of free fall particles in a vertical standpipe was measured by a Laser method [3]. These studies reveal that non-uniformity of particle density occurs in the flow direction when the particle flow rate is high. However, these studies have been conducted with respect to the pipe axial direction rather than with respect to the pipe cross-section. Meanwhile, a cluster formation of particles in a circulating fluidized bed, which is an extreme case of non-uniformity, has been visualized with respect to both the pipe axial direction and the pipe cross-section by the Laser sheet method [4]. However, cluster formation in the cross-section was visualized from an inclined viewpoint and was not estimated quantitatively.

Against this background, the process tomography method has been developed in order to visualize particle behavior in multi-phase flow in pipe cross-section non-invasively and quantitatively [5]. This CT method was applied to gas-solid flow in a pipeline in order to visualize the particle density distribution in the pipe cross-section in time series [6]. Takei et al. have decomposed the CT images with an image processing technique of wavelet multiresolution to point out non-uniform distribution of the particle density not only in the flow direction but also in the cross-section[7]. However, combination of CT and image processing raises a new issue: how to evaluate non-uniformity of the time transitional particles from the time discretized CT images by means of a mathematical method.

In other fields related to fluid engineering, the state transition matrix method is quite often used as a method to evaluate a time transitional relationship between time responses. For instance, the

state transition matrix method is introduced in order to evaluate the vibration response between coolant flow and a fluid structure of a nuclear reactor [8]. This method is used also to calculate the deposition process of sputtered neutral particles in a chemical reaction chamber [9]. Generally, the state transition matrix has been used in such one-dimensional time transitional relationships, but it has not been applied to three-dimensional image fields consisting of two-dimensional space x and y in the one-dimensional time.

In the present study, the state transition matrix is defined in order to evaluate particle density images among discretized CT images. The state transition matrix is applied to CT images of fine and coarse free-fall-particles in a vertical pipe for evaluating the time transitional particle density distribution.

2 THEORY OF STATE TRANSITION MATRIX TO CT IMAGES

A standard cross-section in Figure 1 depicts free fall particle movement in a corrdinate system of a pipe. The particle density changes at a position between a standard cross-section at time t and a cross-section at $t+\Delta t$ by two factors which are space interaction and time transition. The governing equation is assumed to be a Helmholtz type differential equation, which expresses particle movement in the cross-section for a given time t:

$$\nabla^2 U + \alpha \frac{\partial U}{\partial t} + \beta \frac{\partial^2 U}{\partial t^2} = -\rho \tag{1}$$

where U is the particle density distribution with 2D-space x and y, and time t in the cross-section, α and β are coefficients with dimension [t/m^2] and [t^2/m^2], respectively. For α =0, equation (1) is called wave equation, and for β=0, equation (1) is called diffusion equation. This study assumes that the particle diffusion is dominant rather than the particle wave in a free fall particles in a pipe, which expresses β=0. In equation (1), ρ is source density, which is dependent on the space and time. The first term in equation (1) indicates spatial dispersion, and the second term indicates time transition of particle density. After $\nabla^2 U$ is discretized by a discretization method, equation (1) is rewritten as:

$$\mathbf{C}\boldsymbol{U}_t + \gamma \frac{d}{dt}\boldsymbol{U}_t = \boldsymbol{K} \tag{2}$$

$\boldsymbol{U}_t$ is $1\times n^2$ vector when both image space resolution in x and y directions are n. $\mathbf{C}$ is a discretization coefficient of $n^2\times n^2$ matrix, which are composed of coefficients of U. In the case of nine-point finite difference method and zero Dirichlet boundary condition, the relationship between continuous and discrete systems are:

$$\frac{\partial^2 U_{i,j}}{\partial x^2} + \frac{\partial^2 U_{i,j}}{\partial y^2} \approx \frac{1}{6\Delta h}\left[U_{i-1,j-1} + U_{i-1,j+1} + 4U_{i-1,j} + U_{i+1,j+1} + U_{i+1,j-1} + 4U_{i,j+1} + 4U_{i,j-1} - 20U_{i,j}\right]$$

where, i and j are the x and y position in the cross-section. In equation (2), γ and $\boldsymbol{K}$ are:

$$\gamma = \Delta h^2 \alpha \,,\quad \boldsymbol{K} = -\Delta h^2 \boldsymbol{\rho}$$

where Δh is a distance between the discrete grids. $\boldsymbol{K}$ is dependent on $\boldsymbol{\rho}$, which is source density $1\times n^2$ vector. Based on equation (2), the continuous particle density U in equation (1) becomes the discrete particle density $\boldsymbol{U}_t$, which is dependent on time only. Multiplying equation (2) by γ^{-1} yields

$$\frac{d}{dt}\boldsymbol{U}_t = -\mathbf{A}\boldsymbol{U}_t + \boldsymbol{F} \tag{3}$$

where, $\mathbf{A} = \gamma^{-1}\mathbf{C}$ and $\boldsymbol{F} = \gamma^{-1}\boldsymbol{K}$. In equation (3), $\mathbf{A}$ is the state transition value matrix governing the particle density transition, which is $n^2\times n^2$ matrix, and $\boldsymbol{F}$ is a $1\times n^2$ input vector. Because equation (3) cannot be resolved directly, mode coordinates are considered. The mode matrix

consisting of the eigen-vector of $\mathbf{A}$ is replaced by $\mathbf{Z}$, and $\boldsymbol{U}_t$ is rewritten using linear coupling between the element of $\mathbf{Z}$ and the element of vector $\boldsymbol{Y}$:

$$\boldsymbol{U}_t = \mathbf{Z}\boldsymbol{Y} \tag{4}$$

where, $\mathbf{Z} = [\boldsymbol{z}_1, \boldsymbol{z}_2, \boldsymbol{z}_3, \cdots \boldsymbol{z}_{n\times n}]$, $\boldsymbol{z}_1$ is a transpose vector of 1st eigen-vector of $\mathbf{A}$. After equation (4) is substituted into equation (3), the equation (3) is rewritten as:

$$\frac{d}{dt}\boldsymbol{Y} = -\boldsymbol{\Lambda}_p\boldsymbol{Y} + \mathbf{Z}^T\boldsymbol{F} \tag{5}$$

where, $\mathbf{Z}^{-1} = \mathbf{Z}^T$ because $\mathbf{Z}$ is an orthonormal matrix, and $\boldsymbol{\Lambda}_p = \mathbf{Z}^T\mathbf{A}\mathbf{Z}$. $\boldsymbol{\Lambda}_p$ is the transition matrix of the real physical system indicating particle density transition, which is a square matrix with diagonal elements of the eigen-values of $\mathbf{A}$. The solution vector of the modal equation (5) is:

$$\boldsymbol{Y}_t = \boldsymbol{\Lambda}_p^{-1}\mathbf{Z}^T\boldsymbol{F} + e^{-\boldsymbol{\Lambda}_p t}\left(\boldsymbol{Y}_0 - \boldsymbol{\Lambda}_p^{-1}\mathbf{Z}^T\boldsymbol{F}\right) \tag{6}$$

where, $\boldsymbol{Y}_0$ is the initial vector. When the vector from the input vector $\boldsymbol{F}$ is replaced with $\boldsymbol{Y}_f$, equation (6) is rewritten as:

$$\boldsymbol{Y}_t = \boldsymbol{Y}_f + e^{-\boldsymbol{\Lambda}_p t}(\boldsymbol{Y}_0 - \boldsymbol{Y}_f) \tag{7}$$

Because $\mathbf{Z}e^{-\boldsymbol{\Lambda}_p t} = e^{-\boldsymbol{\Lambda}_p t}\mathbf{Z}$, when $\mathbf{Z}$ multiplies equation (7) from the left side,

$$\boldsymbol{U}_t = \boldsymbol{U}_f + e^{-\boldsymbol{\Lambda}_p t}\left[\boldsymbol{U}_0 - \boldsymbol{U}_f\right] \tag{8}$$

is obtained. The equation (8) means the density distribution $\boldsymbol{U}_t$ at an arbitrary time t is expressed by the first particle density distribution $\boldsymbol{U}_0$ and the final particle density distribution $\boldsymbol{U}_f$.

In equation (8), in the case of t =0, the intermediate density distribution $\boldsymbol{U}_t$ is equal to the initial density distribution $\boldsymbol{U}_0$, in the case of $t \to \infty$, the intermediate density distribution $\boldsymbol{U}_t$ is equal to the final density distribution $\boldsymbol{U}_f$. When equation (8) is applied among three discretized CT images, the following relation holds:

$$\boldsymbol{U}_{i+1} = \boldsymbol{U}_{i+2} + e^{-\boldsymbol{\Lambda}\Delta t}\left[\boldsymbol{U}_i - \boldsymbol{U}_{i+2}\right] \tag{9}$$

where i is the frame number of CT images, Δt is the time resolution of CT images. The state transition matrix in the image system $\boldsymbol{\Lambda}$ indicates the transition quantities among three images. On the basis of equation (9), the state transition matrix Λ is rewritten as:

$$\boldsymbol{\Lambda} = \frac{-1}{\Delta t}\ln\left[\frac{\boldsymbol{U}_{i+1} - \boldsymbol{U}_{i+2}}{\boldsymbol{U}_i - \boldsymbol{U}_{i+2}}\right] \tag{10}$$

where, $\boldsymbol{\Lambda}$ is a $n^2 \times n^2$ diagonal matrix of eigen-values λ; however, the element position is replaced with column and row order to easily visualize the transition as an image:

$$\boldsymbol{\Lambda} = \begin{bmatrix} \lambda_1 & & & \\ & \lambda_2 & & 0 \\ & & \ddots & \\ & 0 & & \lambda_{n\times n-1} \\ & & & & \lambda_{n\times n} \end{bmatrix} \Rightarrow \boldsymbol{\Lambda} = \begin{bmatrix} \lambda_1 & \lambda_1 & \cdots & \lambda_1 & \lambda_n \\ \lambda_{n+1} & & \cdots & & \\ & & \cdots & & \\ & & \cdots & & \\ & 1 & \cdots & \lambda_{n\times n-1} & \lambda_{n\times n} \end{bmatrix}$$

When $\boldsymbol{\Lambda}$ is calculated, the particle movement characteristic among three images is extracted as linear or non-linear.

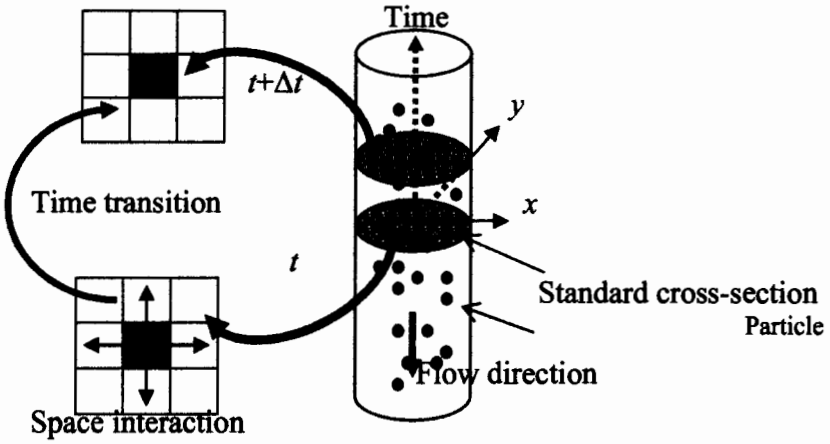

Figure 1 Coordinate system in a pipe and particle density factors.

3 EXPERIMENTS

Figure 2 shows the experimental equipment, which is composed of a hopper for supplying particles, a vertical pipe, the CT sensor (Yang 1996), and a receiver. The pipe is 2m long and has an inside diameter of 50 mm. Polyethylene pellets are dropped in freefall from the hopper at four flow rates, which are $Q_1=3.08\times10^{-5}$ m^3/s, $Q_2=1.27\times10^{-4}$ m^3/s, $Q_3=2.80\times10^{-4}$ m^3/s and $Q_4=5.56\times10^{-4}$ m^3/s. Mean diameters of coarse and fine particles are 3.26 mm and 1.75×10^{-4} mm. The obtained images consist of 350 frames obtained at 100 Hz interval; namely, Δt is 10 milliseconds.

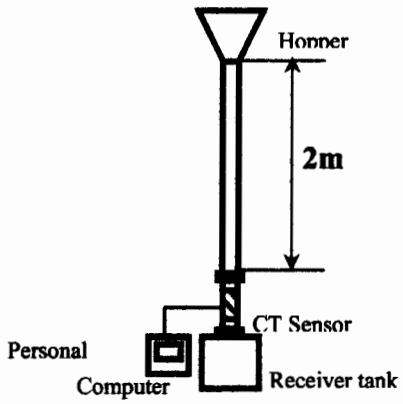

Figure 2 Experimental equipment.

4 IMAGE PROCESSING AND DISCUSSION

In order to clarify the density transition in the pipe cross-section, a transition pattern map among three discrete images at a given time was produced. The process to produce the map is as follows: First, three images $\boldsymbol{E}$ in time order are substituted into $\boldsymbol{U}$ in equation (10) in order to obtain the transition matrix $\boldsymbol{\Lambda}$. Second, on the basis of the value pattern of $\boldsymbol{\Lambda}$, the dominant density transition pattern; namely, monotonous transition, sudden transition or extreme value transition is judged. from Table 2. Third, the transition pattern map in the pipe cross-section is produced by binarizing the density transition pattern; namely, when sudden transition is extracted, the pixel of the sudden

transition is replaced with 1.0, which is indicated by white; moreover, the pixel of the other transition or non-transition is replaced with 0.0. On the other hand, when extreme value transition is extracted, the pixel of the extreme transition is replaced with 1.0; moreover, the pixel of the other transition or non-transition is replaced with 0.0. Finally, the process from the first step to the third step is repeated for all images in time sequence. As a result, the positions where the kinds of transition patterns occur in the cross-section are qualitatively visualized. The characteristics of the state transition matrix have already reported [12]. Figure 3 is the time-mean transition pattern map obtained from the total time in the case of coarse particles. Figure 4 is the time-mean transition pattern map obtained from the total time in the case of fine particles. In both figures, (1) is the sudden transition, and (2) is the extreme value transition. The red region indicates high intensity of the transition, and the blue region indicates low intensity of the transition. According to the figure 3, which is coarse particles, in the case of low particle flow rate Q_1, the high sudden and extreme value transitions (red region) slightly occurs near the pipe wall mainly. In the case of intermediate particle flow rate Q_2 and Q_3, the intensity of the sudden and extreme value transitions (red region) relatively increases near the pipe center. In the case of high particle flow rate Q_4, the sudden transition and the extreme value transition strongly occurs on the whole. On the other hand, the fine particles patterns are different from the fine particles. According to figure 4, which is fine particles, in the case of low particle flow rate Q_1, the high sudden and extreme value transitions (red region) slightly occurs near the pipe center mainly. In the case of intermediate particle flow rate Q_2 and Q_3, the intensity of the sudden and extreme value transitions (red region) relatively increases near the pipe wall. In the case of high particle flow rate Q_4, the sudden transition and the extreme value transition strongly occurs on the whole.
First, the relationship between the particle pattern and the particle flow rate are discussed in the both figures 3 and 4. In free falling particles in a pipeline, so-called inhomogeneous particle density is reported. In the case of large particle size, such as that used in this study, the dominant factor for inhomogeneous particle density becomes particle collision rather than turbulence. This means that the particle density becomes inhomogeneous because the particles collide with one another and with the wall.
Next, the difference between coarse and fine particles in the case of the low particle flow rate Q_1 is discussed. Generally, coarse particles tend to move out more in a cross section when the particles collide than fine particles because the momentum of coarse particles is higher than that of the fine particles.

Figure 3 Time mean transition patterns of coarse particles.

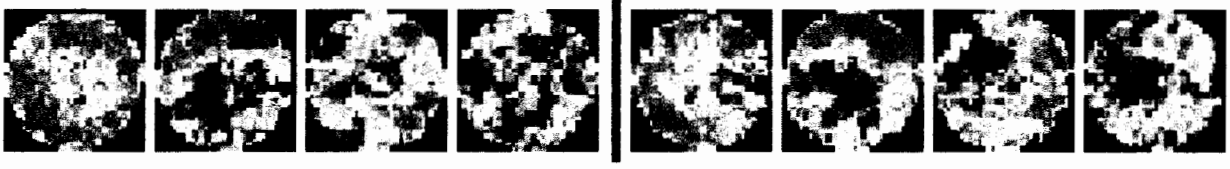

Figure 4 Time mean transition patterns of fine particles.

5 CONCLUSIONS

The state transition matrix Λ has been defined from the Helmholtz type differential equation to apply to evaluation of particle transitional process. Λ is applied to coarse and fine free-fall-particles density distribution images visualized by CT sensor in order to discuss the particle transition patterns. The following results are obtained:

(1) In the case of coarse particles, sudden transition and extreme value transitions does not occur frequently when particle flow rate is low. However, the transitions occur at the pipe center when the flow rate is high because the probability of collision among particles is high.

(2) In the case of fine particles, the high sudden and extreme value transitions slightly occur near the pipe center mainly in the case of low particle flow rate. Moreover, the sudden and extreme value transition strongly occurs on the whole in high particle flow rate,. That is because the momentum of coarse particles is higher than that of the fine particles.

6 REFERENCES

1. Fessler, J. R., Kulick, J. D. and Eaton ,J. K., 1994, Preferential concentration of heavy particles in a turbulent channel flow, *Phys. Fluids* 6(11): 3742-3749.
2. Isaksen, O., 1996, A review of reconstruction techniques for capacitance tomography, *Measurement science & technology* 7(3): 325-337.
3. Wang, Q. and Squires, K. D., 1996, Large eddy simulation of particle-laden turbulent channel flow, *Phys. Fluids* 8(5): 1207-1223.
4. Peng, G. and Herrmann, H. J., 1995, Density waves and 1/f density fluctuations in granular flow, *Physical Review E* 51(3): 1745-1756.
5. Horio, M. and Kuroki, H., 1994, Three-dimensional flow visualization of dilute dispersed solids in bubbling and circulating fluidized beds, *Chemical Engineering Science* 49(15): 2413-2421.
6. Huang, S. M., Plaskowski, A. B., Xie, C. G. and Beck, M. S., 1989, Tomographic imaging of two-component flow using capacitance sensors, *Journal Physics E: Sci, Intrrum* 22: 173-177.
7. Dyakowski, T., Luke, S. P., Ostrowski, K. L. and Williams, R. A., 1999, On-line monitoring of dense phase flow using real time dielectric imaging, *Powder technology* 104: 287-295.
8. Takei, M., Li, H., Ochi, M., Saito, Y., Horii, K., 2002, Feature extraction of particle density in a pipeline with tomography and wavelets, *International Journal Applied Electromagnetics and Mechanics,* 15, pp.423-430.
9. Kuzelka, V., 1982, A solution of the vibrational response reactor components to random exciting forces due to coolant flow, *Nucear engineering and design.* 72(2): 189-196.
10. Parker, G. J., Hitchon, W. N. G. and Koch, D. J., 1995, Transport of sputtered neutral particles, *Physcal Review.E* 51(4): 3694-3703.
11. Isaksen,O., 1996, A review of reconstruction techniques for capacitance tomography, *Measurement science & technology* 7(3): 325-337.
12. Yang, W. Q., 1996, Hardware design of electrical capacitance tomography systems, *Measurement science & technology* 7(3): 225-232.
13. Takei, M., Li, H., Ochi, M., Saito, Y., Horii, K., 2003, Evaluation of Free Fall Particle CT Images Using State Transition Matrix, *Particulate Science and Technology Journal,* 21(1) (in press)